Front. Mater. Sci. 2021, 15(1): 79–97
https://doi.org/10.1007/s11706-021-0541-0

REVIEW ARTICLE

Recent progress in graphene-reinforced aluminum matrix composites

Jinlong SU and Jie TENG (✉)

College of Materials Science and Engineering, Hunan University, Changsha 410082, China

ABSTRACT: Recent years witnessed a growing research interest in graphene-reinforced aluminum matrix composites (GRAMCs). Compared with conventional reinforcements of aluminum matrix composites (AMCs), graphene possesses many attractive characteristics such as extremely high strength and modulus, unique self-lubricating property, high thermal conductivity (TC) and electrical conductivity (EC), and low coefficient of thermal expansion (CTE). A lot of studies have demonstrated that the incorporation of graphene into Al or Al alloy can effectively enhance mechanical and physical properties of the Al matrix. The purpose of this work is aimed to trace recent development of GRAMCs. Initially, this paper covers a brief overview of fabrication methods of GRAMCs. Then, mechanical, tribological, thermal and electrical properties of recently developed GRAMCs are presented and discussed. Finally, challenges and corresponding solutions related to GRAMCs are reviewed.

KEYWORDS: graphene; aluminum; metal matrix composite; mechanical properties; tribological properties

Contents

Received September 3, 2020; accepted December 8, 2020

E-mail: tengjie@hnu.edu.cn

1 Introduction

Aluminum matrix composites (AMCs) are synthesized by incorporating a certain content of reinforcement phases into Al or Al alloy matrix. As a branch of metal matrix composites (MMCs), AMCs have been widely investigated in previous studies [1–2]. The merits of Al and Al alloy are their low density, high specific strength, excellent wear resistance, and good corrosion resistance [3–4]. To obtain desired performance, a new generation of nano-sized reinforcement phase, graphene, has been adopted for strengthening AMCs.

Graphene, one of the most important carbonaceous nanomaterials, is a single atom layer made by carbon atoms hybridizing sp^2. In graphene, carbon atoms are densely packed in a honeycomb/hexagonal lattice structure. The properties of single-layer graphene are listed in Table 1 [4–10]. The ultimate tensile strength (UTS) and the elastic modulus of graphene are 130 GPa and 1 TPa, respectively [6]. In terms of physical properties, graphene possesses excellent thermal conductivity (TC; 1000–5000 $W \cdot m^{-1} \cdot K^{-1}$) and room temperature electron mobility (~2.0×10^5 $cm^2 \cdot V^{-1} \cdot s^{-1}$). Furthermore, the unique two-dimensional (2D) structure endows it an extremely high specific surface area (2630 $m^2 \cdot g^{-1}$) [11]. Due to these interesting characteristics, the research related to graphene-reinforced aluminum matrix composites (GRAMCs) grew vigorously within past decade.

Graphene-related materials, such as graphene nanoplatelets (GNPs) and graphene nanosheets (GNSs), have been investigated intensively as the reinforcement of AMCs because of their ease of production and high cost-effectiveness [12]. GNPs and GNSs are stacks of multi-layer graphene sheets with an average thickness of 5–100 nm. Due to that the single-layer graphene is not stable in the state of freedom, GNPs and GNSs are more frequently used in AMCs. In some cases, GNPs and GNSs can be peeled into few-layer graphene (FLG) or single-layer graphene in the subsequent manufacturing process [13].

Moreover, some derivatives of graphene, such as graphene oxide (GO) and reduced graphene oxide (RGO), can also be used as reinforcements for AMCs. The chemical structures of GO and RGO are presented in Fig. 1 [14]. GO possesses a honeycomb/hexagonal structure, which resembles graphene but contains many functional groups, e.g., hydroxyl (OH), alkoxy (COC), carbonyl (CO), and carboxylic acid (COOH). These functional groups result in a hydrophilic nature of GO. However, the studies related to GO-reinforced AMCs are few due to the alumina (Al_2O_3) formation during the manufacturing process. RGO, prepared by the chemical reduction of GO, is frequently used in AMCs. As shown in Fig. 1(b), the structure of RGO is also similar to graphene, but contains residual functional groups and structural defects at the edge [15].

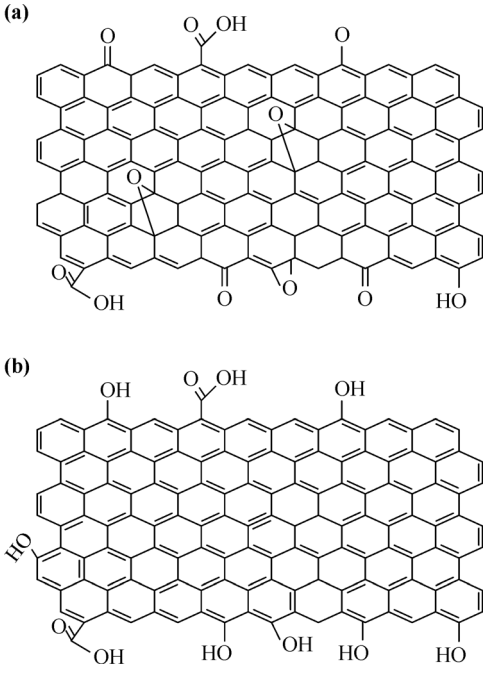

Fig. 1 Chemical formulae of **(a)** GO and **(b)** RGO. Reproduced with permission from Ref. [14].

The merits of GRAMCs are their superior mechanical properties and excellent wear resistance. Moreover, the improvement in electrical conductivity (EC) and TC has also been reported in comparison with unreinforced alloy [10,16]. However, the development of GRAMCs is still in

Table 1 Properties of pure Al and single-layer graphene [4–10]

Material	Properties							
	UTS/MPa	η/GPa	ρ/($g \cdot cm^{-3}$)	T_m/°C	EC/($S \cdot m^{-1}$)	A_s/($m^2 \cdot g^{-1}$)	TC/($W \cdot m^{-1} \cdot K^{-1}$)	CTE/K^{-1}
Al	80	70	2.7	660	3.2×10^7	–	237	$(21–24) \times 10^{-6}$
Single-layer graphene	1.3×10^5	1.0×10^3	1.06	5727	9.6×10^7	2630	1000–5000 [a]	-8.0×10^{-6} [b]

Notes: η, elastic modulus; ρ, density; A_s, specific surface area; CTE, coefficient of thermal expansion; EC, electrical conductivity; TC, thermal conductivity; T_m, melting point; UTS, ultimate tensile strength.
a) In-plane; b) Room temperature.

the laboratory stage. The existing challenges can be divided into following aspects: (i) inhomogeneous dispersion of graphene; (ii) weak interfacial bonding and carbide formation; and (iii) structure integrity. To overcome such difficulties, many novel strategies have been executed in the past few years. In this review, recent progress in the fabrication of GRAMCs and their properties are presented and discussed. The properties of GRAMCs discussed cover mechanical, tribological, electrical and thermal properties. In addition, this review comprehensively discusses the challenges related to GRAMCs and the recently developed strategies.

2 The fabrication of GRAMCs

2.1 Powder metallurgy

Benefiting from the near-net formability and uniformity of the reinforcement distributions, powder metallurgy (PM) processing techniques are preferred methods for the synthesis of GRAMCs. Generally, PM processing techniques involve two stages, mixing powder and consolidation. Through appropriate processing parameters, uniform dispersion of reinforcements and superior mechanical properties of composites can be achieved. Nevertheless, the major disadvantage of PM is the oxidation of the metal matrix and the unclean interfaces between Al and graphene.

2.1.1 Mixing powder

Initially, the dispersion degree of graphene strongly depends on the mixing stage. In general, the mixing methods can be divided into ball milling and solution mixing. Through one or both, graphene can be effectively dispersed in the Al matrix.

Among all milling methods, shaker ball milling and planetary ball milling are commonly used. In addition to room temperature milling methods, the cryomilling method is also an effective approach that could promote the dispersion of reinforcements and result in a higher strengthening effect [17]. The advantages and disadvantages of several ball milling methods are listed in Table 2. For the ball milling methods, the quality of mixing stage depends on milling time, ball-to-powder weight ratio and rotation speed/frequency. Besides, milling balls, jars, process control agents (PCAs) and milling atmosphere also influences the dispersion of reinforcements. Generally, longer milling time, larger ball-to-powder weight ratio and higher rotation speed result in a higher energy input, which is beneficial to the dispersion of reinforcements. However, excessive energy input could lead to the severe cold welding of powders, the formation of Al_4C_3 and the destruction of structural integrity of graphene, which deteriorates the properties of composites [18–19]. As a result, proper milling parameters are essential for achieving a balance between dispersion and structural integrity of graphene. Yu et al. [18] investigated the effect of ball milling time (1–4 h) on the dispersibility of Al6063/GNSs powders, and the results indicated that various dispersion characteristics were obtained with different ball milling time. As depicted in Figs. 2(a) and 2(b), the morphology of mixed powders was of equal-axis and most of the GNSs were distributed between Al powders when the milling time is 1 h. When the milling time is 2 h, the morphology of powders transformed to flake-shape and most of the GNSs were dispersed on the surface of Al6063 powders, as depicted in Figs. 2(c) and 2(d). Increasing the milling time to 3 h, some of the flake-shape powders were cold-welded and the GNSs were distributed inside the Al6063 powders. Further increasing the milling time to 4 h result in more severe cold welding, and flake-shape powders and Al_4C_3 carbides were formed in the mixed powders.

Solution mixing is a method of stirring or sonicating mixture containing metal powders and graphene particles [20]. For solution mixing, the dispersion effect strongly depends on mixing method (ultrasonic and/or mechanical mixing), mixing speed/frequency, mixing time and solution. Compared with ball milling, the merit of solution mixing is that it can get uniform dispersion without destroying the structural integrity of graphene. Moreover, contamination issue of mixing powders and formation of Al_4C_3 carbides can be avoided. In our previous work, a

Table 2 Advantages and disadvantages of several ball milling methods

Method	Advantages	Disadvantages
Shaker ball milling	high energy input and time-saving	low production rate; risk of contamination and formation of Al_4C_3
Planetary ball milling	high productivity and cost-effectiveness	risk of contamination and formation of Al_4C_3
Cryomilling	achievement of grain refinement; suppression of recovery and recrystallization; reduced usage of PCA, resulting in less contamination and a clean interface	high cost

homogeneously dispersed graphene/Al composite were obtained through a solution mixing and powder metallurgy method [20]. During the manufacturing process, aqueous GO suspension was prepared through a modified Hummer's method at the initial stage. Then, Al powders were mixed with the GO suspension, followed by ultrasonic mixing and mechanical stirring to obtain homogeneous slurry. After the slurry was dried, the uniform mixture of Al/GO powders was obtained, as shown by the scanning electron microscopy (SEM) image in Fig. 3(b). Next, the powder mixture was heated at 550 °C for 2 h to reduce GO to RGO. Finally, through a pre-sintering and hot extrusion process, the Al/RGO composites with a uniform dispersion of RGO were achieved. This mixing method not only utilizes the hydrophilicity of GO to obtain a uniform dispersion of reinforcements but also avoided the formation of Al_2O_3 and Al_4C_3. With the incorporation of 0.3 wt.% RGO, an 25.6% enhancement in UTS is obtained relative to pure Al.

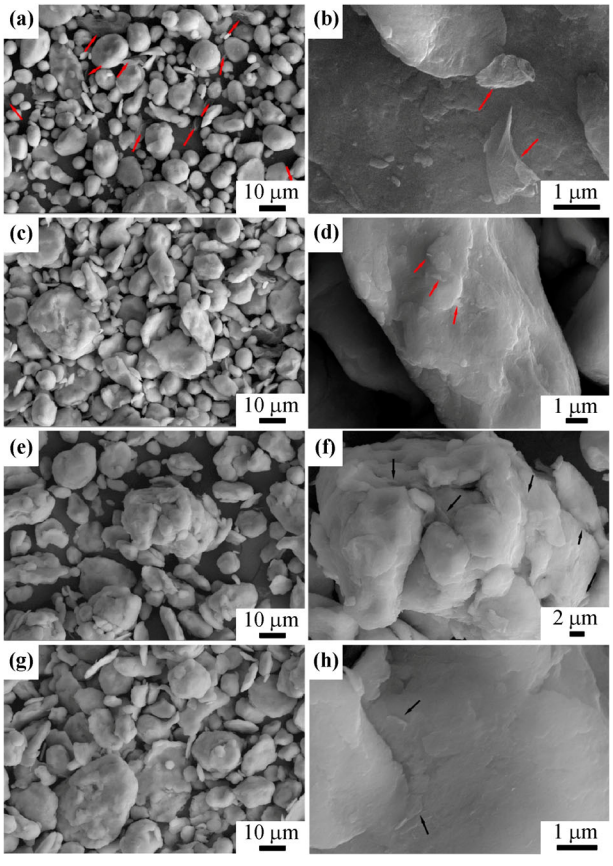

Fig. 2 SEM images of mixed Al/GNSs powders with different milling time: **(a)(b)** 1 h; **(c)(d)** 2 h; **(e)(f)** 3 h; **(g)(h)** 4 h. Reproduced with permission from Ref. [18].

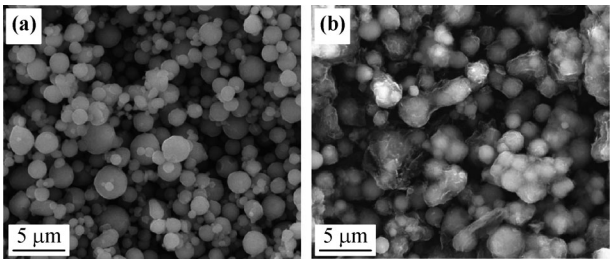

Fig. 3 SEM images of **(a)** Al powders and **(b)** mixed Al/GO powders. Reproduced with permission from Ref. [20].

2.1.2 Consolidation

After the power mixture was obtained, a consolidation step was executed to fabricate a bulk composite. Although the dispersion of graphene cannot be affected by the consolidation process, the comprehensive properties of the GRAMCs strongly depend on the consolidation process [12]. The consolidation methods used in GRAMCs generally involve conventional sintering, hot press sintering (HPS), hot isostatic pressing (HIP), microwave sintering (MWS), and spark plasma sintering (SPS). The advantages and disadvantages of these consolidation methods are summarized in Table 3. In some cases, secondary processing methods, e.g., hot rolling, hot extrusion, and friction stir processing (FSP), are adopted for further reducing the porosity and promoting the dispersion of graphene [21].

2.2 Casting

In casting methods, the GRAMCs were fabricated through mixing graphene with Al melt. The stir casting is the most

Table 3 Advantages and disadvantages of several consolidation methods

Method	Advantages	Disadvantages
Conventional sintering	low cost and high production rates; formation of complex shapes	poor densification and long dwell time
HPS	better densification than conventional sintering	long dwell time
HIP	uniform densification and isotropic properties	long dwell time
MWS	higher heating rates, shorter sintering time relative to conventional sintering	poor densification relative to SPS
SPS	high heating rates, short dwell times, low porosity and excellent mechanical properties	high cost

Notes: HIP, hot isostatic pressing; HPS, hot pressing sintering; MWS, microwave sintering; SPS, spark plasma sintering.

frequently method used for fabricating MMCs among casting methods. In comparison with solid-phase processing, the merits of liquid-phase processing are more economical and scalable for mass-production [22–24].

However, there are relatively few studies related to the casting of GRAMCs compared with PM methods. It is known that the wettability between Al and graphene is poor and the density of Al and graphene exhibits a large difference, resulting in the agglomeration of graphene in most cases. Das et al. [25] reported an innovative pressure infiltration method by incorporating Ni spheres into the preform. In their study, Ni spheres were incorporated into graphene to form the preform, and the A356 alloy melt was infiltrated into the preform to fabricate the composites. The results indicate that the wettability between Al and graphene is enhanced effectively due to the formation of Ni–Al intermetallic phase on the surface of Ni spheres. Another challenge related to casting of GRAMCs is that the interfacial reaction between Al and graphene is inevitable due to the high processing temperature, which generally deteriorates the mechanical properties [26]. For this reason, the research related to the casting of GRAMCs is relatively few. In the authors' view, the research related to the interfacial reaction mechanism between Al and graphene during the casting process is still needed to be further investigated.

2.3 Severe plastic deformation

In addition to conventional deformation processes (e.g., extrusion and rolling), severe plastic deformation (SPD) was an attractive technique for improving the density of the consolidated materials due to the extensive plastic deformation [27]. The merits of SPD methods generally involve significant grain refinement of alloy matrix and homogeneous dispersion of reinforcements [13,28–29]. In previous studies, FSP and high-pressure torsion (HPT) have been used for fabricating GRAMCs [13,28–29].

2.3.1 Friction stir processing

In the FSP method, Al matrix and graphene were stirred to form a composite through a non-consumable rotating tool, and the heat and SPD generated by the frictional process facilitate the fabrication of GRAMCs. Compared with typical processing techniques (e.g., PM and casting), the FSP generally involves a more uniform dispersion of reinforcements [26]. Moreover, graphite particles can be exfoliated into single-layer graphene and multi-layer graphene during the FSP due to the very high shear strains of FSP [13]. However, the limitation of the FSP method is that it is not suitable for the production of large-scale bulk composite materials and the control of composition is difficult. A typical schematic representation of the FSP setup is presented in Fig. 4 [26]. Sharma et al. [26] proposed a multiple micro channel reinforcement filling (MMCRF) strategy for fabricating Al6061/GNPs composite through FSP. The results indicate that the MMCRF strategy can make GNPs more evenly dispersed within the composite with relative to the conventional single channel reinforcement filling.

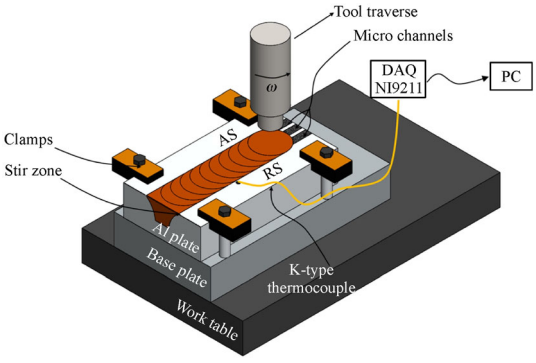

Fig. 4 Schematic representation of the FSP setup. Reproduced with permission from Ref. [26].

2.3.2 High-pressure torsion

Compared with conventional processing techniques (e.g., PM and casting), the HPT processing is characterized by its low processing temperature, which could avoid the formation of alumina and carbide. In the HPT method, the processing temperature used for fabricating MMCs is between 298 and 473 K, obviously lower than typical sintering temperatures for Al alloys [29]. Huang et al. [29] investigated the fabrication of the Al/5 wt.% GNPs composite by HPT at the temperature range of 298–473 K. It was found that the GNPs agglomerations were fragmented gradually and uniform dispersion of GNPs within Al matrix was achieved with the increasing HPT turns. Moreover, significant grain refinement of the composite was achieved through HPT. After processing at 298 and 473 K for 20 turns, the grain sizes of the Al matrix reached 70 and 155 nm, respectively.

2.4 Additive manufacturing

Additive manufacturing, namely three dimensional (3D) printing, has received many researchers' attention in recent

years due to its unique capability to fabricate complex parts quickly [30–35]. It should be noted that the plasticity of GRAMCs generally tends to deteriorate with the addition of graphene, which makes it difficult for GRAMCs to be processed into complex parts. At this point, additive manufacturing is an attractive approach for obtaining complex parts of GRAMCs directly. Hu et al. [31] fabricated Al/x graphene (x = 0.5, 1.0 and 2.5 wt.%) through ball milling combined with selective laser melting (SLM). In their study, agglomeration of graphene occurred when the graphene content reached 2.5 wt.%. To promote the dispersion of graphene, Zhao et al. [36] proposed a novel activating treatment of coating a nano-Al layer on the graphene surface, namely organic aluminum reduction. After the activating treatment, a homogeneously dispersed 1 wt.% graphene/AlSi10Mg composite was successfully fabricated through SLM. Tiwari et al. [33] investigated the effect of graphene content and laser power on the AlSi10Mg/graphene composites through powder bed fusion. The schematic diagram of the processing route of AlSi10Mg/graphene composites is presented in Fig. 5 [33]. It was found that the laser power required for the appropriate melting of AlSi10Mg/graphene composite powders was higher than that of the AlSi10Mg alloy. In above studies, the hardness and the yield tensile strength (YTS) of GRAMCs are increased with the incorporation of graphene. However, the ductility generally tends to decrease, which is caused by the Al_4C_3 phase formation due to the high processing temperature of SLM [37].

3 Comprehensive comments on currently investigated GRAMCs

3.1 Mechanical behavior

3.1.1 Strengthening mechanism

The mechanical properties of GRAMCs are influenced by many factors, such as the composition of alloy matrix, processing parameters, distribution, size and structural integrity of graphene, and carbide formation. Generally, the strengthening mechanisms of GRAMCs include following aspects: (i) load transfer from matrix to reinforcements; (ii) grain refinement due to the pinning effect by reinforcements; (iii) mismatch in coefficient of thermal expansion (CTE) between the alloy matrix and reinforcements; and (iv) Orowan strengthening.

Due to the large volume fraction of the Al/graphene interface area within GRAMCs, the load transfer mechanism is commonly found in GRAMCs. The load transfer efficiency strongly depends on the interfacial bonding between Al and graphene. The Keely–Tyson formula has been widely adopted to evaluate the UTS of GRAMCs [38]:

$$\sigma_c = \sigma_f V_f \cdot \frac{l}{2l_c} + \sigma_m(1-V_f) \quad (l < l_c) \tag{1}$$

$$\sigma_c = \sigma_f V_f \left(1-\frac{l_c}{2l}\right) + \sigma_m(1-V_f) \quad (l \geqslant l_c) \tag{2}$$

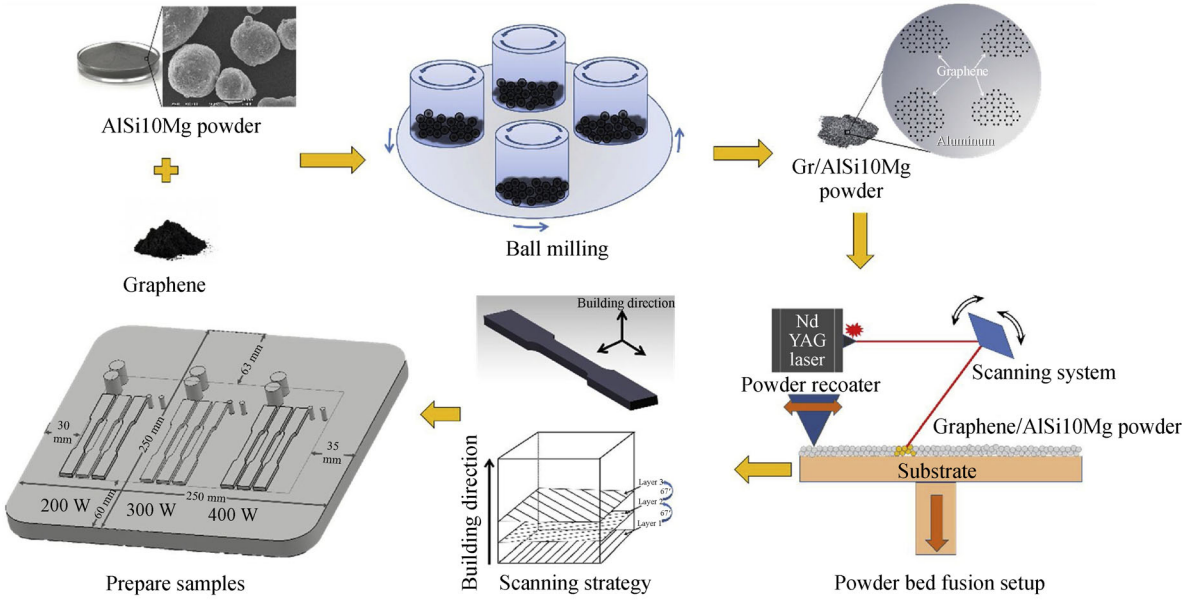

Fig. 5 Schematic diagram of the processing route of the AlSi10Mg/graphene composite. Reproduced with permission from Ref. [33].

where σ_c, σ_f and σ_m are UTS values of the composite, the reinforcement and the metal matrix, respectively; V_f and l are the volume fraction and the average length of the reinforcements, respectively; and $l_c = \sigma_f D/(2\tau_m)$ is the critical length of the fiber, in which D is the fiber diameter and τ_m (= $0.5\sigma_m$) is the shear strength of the metal matrix. When l is larger than or equal to l_c, the fiber is loaded up to its UTS.

The grain refinement strengthening can be explained by the Hall–Petch relationship:

$$\Delta\sigma_{HP} = k_y(D_c^{-1/2} - D_a^{-1/2}) \tag{3}$$

where $\Delta\sigma_{HP}$ is the increment in YTS due to grain refinement; k_y is the Hall–Petch coefficient of the alloy matrix; and D_c and D_a are mean grain sizes of the composite and the alloy matrix (without graphene), respectively.

The large mismatch of CTE between Al and graphene leads to the prismatic punching of dislocations at the Al/graphene interface, thereby strengthening the composites. The CTE mismatch strengthening effect can be evaluated through the following formula:

$$\Delta\sigma_{CTE} = 4.33 G_m b \sqrt{\frac{V_f \Delta T \cdot \Delta CTE}{b d_p}} \tag{4}$$

where $\Delta\sigma_{CTE}$ is the increment in YTS of the composite due to the CTE mismatch; G_m and b are the shear modulus and the burger vector of the alloy matrix, respectively; ΔT is the temperature difference; ΔCTE is the difference in CTE; and d_p is the mean size of reinforcements.

The Orowan strengthening mechanism is caused by restricted movements of dislocations in the alloy matrix due to uniformly distributed reinforcements. When the reinforcements cannot hinder the motion of dislocations and allow them to pass through, dislocation loops are formed, namely “Orowan loops”. The presence of Orowan loops can further hinder the motion of dislocations, thus, the strength of the composite was enhanced. The increment in YTS can be evaluated by the Orowan–Ashby model [39]:

$$\Delta\sigma_{Orowan} = \frac{0.13 G_m b}{d_p\left[\left(\frac{1}{2V_f}\right)^{1/3} - 1\right]} \cdot \ln\left(\frac{d_p}{2b}\right) \tag{5}$$

3.1.2 Mechanical properties

As discussed above, the mechanical properties of GRAMCs show a larger difference even in the same composition, and we will summarize mechanical properties of recently developed GRAMCs prepared by various processing methods in this part. Due to the extremely high UTS (130 GPa) and elastic modulus (1 TPa) of graphene, the theoretical mechanical properties of GRAMCs predicted by the rule of mixture are superior. For instance, the theoretical UTS of Al/0.3 wt.% GNSs composite is as high as 500 MPa with the premise of GNSs aligned along the tensile direction [40]. However, the mechanical properties obtained by tensile tests are significantly lower than the theoretical value. The difference between theoretical and experimental values can be attributed to the inhomogeneous dispersion, the imperfect orientation of graphene and the weak interfacial bonding between Al and graphene.

Obviously, the performance of GRAMCs is influenced by the content of graphene. In general, the incorporation of minor content of graphene will strengthen the composites, while further addition of graphene will deteriorate it. The maximum strengthening efficiency depends on the dispersion degree of graphene, i.e., the mechanical properties of GRAMCs will be significantly decreased if graphene is agglomerated. The agglomeration of graphene not only overshadows its strengthening effect but also generates defects at the Al/graphene interface, resulting in the premature failure of the composites. As a result, the graphene used in GRAMCs is generally less than 2 wt.%. It is worth noting that the incorporation of low content graphene may also obtain the equivalent strengthening effect corresponding to the high reinforcement content of conventional AMCs (e.g., Al/SiC). For instance, Islam et al. [41] reported that only 0.5 wt.% GNP addition into the Al matrix enhanced the hardness of the composites by 36.5%, which is equivalent to the 5 wt.% SiC nanoparticles addition.

The ductility of GRAMCs generally tends to decrease with the incorporation of graphene, as listed in Table 4 [13,17–18,20,22,31,35,42–63]. The strength–ductility trade-off issue in GRAMCs is mainly influenced by the dispersion degree of graphene and the interfacial bonding between Al and graphene. Secondary processing (e.g., hot extrusion, rolling, and FSP) can be used to alleviate the trade-off issue. In some studies, the ductility of the composites has even improved relative to the corresponding alloy matrix due to the homogeneous dispersion of graphene and robust interfacial bonding between Al and graphene [18,44,59]. Moreover, Jiang et al. [64] proposed that the trade-off issue could be tailored by introducing higher volume fraction of Al/GNSs interface through varying the size, the thickness and the content of GNSs.

Table 4 Mechanical properties of GRAMCs prepared by various processing methods [13,17–18,20,22,31,35,42–63]

Consolidation method	Composite [a)]	μ/HV	YTS/MPa	UTS/MPa	δ/%	η/GPa	Ref.
Vacuum hot pressing	Al	–	30	104	12.5	21.2	[61]
	Al/0.5 vol.% GNSs	–	70	223	9.6	17.5	
	Al/1.5 vol.% GNSs	–	205	315	7.3	15.6	
	Al/2.5 vol.% GNSs	–	225	318	4.5	8.3	
Vacuum hot pressing + hot rolling	Al	–	131	161	23.5	–	[62]
	Al/0.5 vol.% Ni-GNSs	–	203	230	17.5	–	
	Al/1.0 vol.% Ni-GNSs	–	237	266	19.1	–	
	Al/1.5 vol.% Ni-GNSs	–	255	279	13.2	–	
	AlCu	70.0	226	244	8.5	–	[63]
	AlCu/1.0 vol.% GNSs	73.8	242	254	7.2	–	
	AlCu/2.0 vol.% GNSs	79.8	260	280	6.3	–	
Vacuum hot pressing + hot forging + FSP	Al2009/1.0GNPs (1-pass FSP)	–	314	398	4	–	[42]
	Al2009/1.0GNPs (2-pass FSP)	–	398	514	10	–	
	Al2009/1.0GNPs (3-pass FSP)	–	378	468	7	–	
	Al2009/1.0GNPs (4-pass FSP)	–	363	462	8	–	
Cold compaction + sintering + hot extrusion	Al	–	67	103	48.2	68.2	[43]
	Al/0.4GNPs	–	64	106	31	63.7	
	Al/2.0GNPs	–	64	117	30	65.6	
	Al	–	193	233	17.4	71.0	[44]
	Al/0.25 vol.% GNSs	–	207	257	17.6	72.5	
	Al/0.5 vol.% GNSs	–	215	287	17.3	74.9	
	Al	59.1	–	203	30.5	–	[20]
	Al/0.3RGO	74.3	–	255	19.2	–	
	Al/0.6RGO	71.3	–	241	13.2	–	
	Al	54.3	88.1	–	20.3	70.41	[45]
	Al/0.5Ni-GNSs	59.9	162.5	–	13.3	77.34	
	Al/1.0Ni-GNSs	63.7	182.1	–	11.1	89.80	
	Al/1.5Ni-GNSs	65.3	204.5	–	10.0	96.82	
	Al/2.0Ni-GNSs	63.6	185.4	–	8.7	93.13	
	Al	85.1	80.5	133.4	25.2	–	[46]
	Al/0.5Cu-graphene	102.1	121.3	189.9	20.3	–	
	Al/0.75Cu-graphene	123.4	140.2	223.5	17.5	–	
	Al/1.0Cu-graphene	109.3	125.5	201.3	12.8	–	
	Al	54.0	138	175	23.5	–	[17]
	Al/1.0Cu-GNPs	87.8	225	278	17.5	–	
	Al/2.5Cu-GNPs	116.5	360	402	10.6	–	
	Al/3.0Cu-GNPs	117.0	316	363	12.8	–	
	Al6061	60	–	–	–	–	[47]
	Al6061/0.25GNSs	68	–	–	–	–	
	Al6061/0.5GNSs	63	–	–	–	–	
	Al	39.3	83.6	130	25.6	–	[48]
	Al/0.7GNPs	61.4	141	197	14.0	–	
	Al	–	–	135	26.0	–	[49]
	Al/0.24Ni-GNPs	–	–	163	31.3	–	
	Al/0.34Cu-GNPs	–	–	180	22.5	–	
Cold compaction + sintering + hot extrusion + cold drawing	Al	–	139	144	0.89	71.8	[43]
	Al/0.4GNPs	–	208	219	0.84	76.7	
	Al/2.0GNPs	–	–	137	0.30	85.5	
	Al	–	141.8	190.4	4.6	–	[50]
	Al/2.0GNPs	–	150.0	187.6	4.3	–	

(*Continued*)

Consolidation method	Composite [a)]	μ/HV	YTS/MPa	UTS/MPa	δ/%	η/GPa	Ref.
SPS	Al	–	51	105	41.9	–	[51]
	Al/0.25GNPs	–	81	148	33.1	–	
	Al/0.5GNPs	–	101	171	29.9	–	
	Al/1.0GNPs	–	48	71	4.4	–	
	Al_{micro}	–	51	105	41.9	85	[52]
	Al_{micro}/0.5GNPs	–	101	171	29.9	89	
	Al_{nano}	–	80	148	6.6	83	
	Al_{nano}/0.5GNPs	–	148	233	5.1	88	
	Al-4Cu	87	78	215	28	–	[53]
	Al–4Cu/0.3RGO	99	115	275	15	–	
	Al–4Cu/0.5RGO	101	129	290	12	–	
	Al–4Cu/0.7RGO	113	133	310	11	–	
	Al–4Cu/1.0RGO	125	139	320	10	–	
Flake PTF	Al2024	–	203	301	15.2	–	[54]
	Al2024/0.4RGO	–	294	439	8.5	–	
Stir casting	Al7075/0.5GNPs	–	–	147.7	14.7	–	[22]
	Al7075/1.0GNPs	–	–	150	14.9	–	
	Al7075/1.5GNPs	–	–	155.1	15.6	–	
	Al7075/2.0GNPs	–	–	139.1	16.0	–	
Continuous casting + hot rolling	Al	37.42	–	114	11	–	[55]
	Al/0.2GNPs	43.6	–	156	4	–	
Pressure infiltration	Al5083	–	156.9	289.9	21.3	72	[56]
	Al5083/GO	–	184.5	282.7	9.0	72.6	
	Al5083/GNPs	–	186.9	331.0	6.3	72.6	
Pressure infiltration + hot extrusion	Al6063	–	–	225.9	14	–	[18]
	Al6063/GNSs	–	–	276.7	14.7	–	
	Al6061	–	334	357	12.1	–	[57]
	Al6061/0.6GNPs	–	389	500	2.1	–	
FSP	Al	31.6	50	84	33	–	[13]
	Al/graphene	48.7	94	147	26	–	
	Al6061/GNPs	–	88.27	111.38	3.73	25.64	[58]
FSP + hot extrusion	Al	–	–	127.2	21.7	–	[59]
	Al/graphene	–	–	149.2	29.3	–	
Deformation-driven processing	Al	–	–	119	20.8	69.1	[60]
	Al/GNPs	–	–	497	15.2	76.9	
SLM	Al	38	–	–	–	–	[31]
	Al/0.5graphene	47.1	–	–	–	–	
	Al/1.0graphene	49.6	–	–	–	–	
	Al/2.5graphene	66.6	–	–	–	–	
	AlSi10Mg	120	–	357	5.5	–	[35]
	AlSi10Mg/1.0graphene	169	–	396	6.2	–	

Notes: η, elastic modulus; μ, micro-hardness; FSP, friction stir processing; PTF, powder thixoforming; SLM, selective laser melting; SPS, spark plasma sintering; UTS, ultimate tensile strength; YTS, yield tensile strength.
a) Except for a few cases, the material chemical compositions are in mass fraction (wt.%).

3.2 Tribological behavior

3.2.1 Tribological mechanism

As discussed above, the hardness of GRAMCs is enhanced by four strengthening mechanisms, i.e., load transfer, grain refinement, mismatch in CTE, and Orowan strengthening. According to the Archard theory, the wear loss of samples caused by adhesive wear is inversely proportional to the hardness as described [65–66]. Therefore, the wear resistance of GRAMCs can also be enhanced through these strengthening mechanisms [67].

More importantly, the coefficient of friction (COF) of GRAMCs can be effectively reduced through the incorporation of GNPs/GNSs/FLG, namely the self-lubricating effect [32,68–69]. During the wear tests, high shear stresses are acted on the worn surface of GRAMCs. At this point, interlayer sliding of GNPs/GNSs/FLG generally took place due to the weak van der Waals interaction between GNSs, thus effectively reducing the frictional force and the COF of GRAMCs. The self-lubricating phenomenon of GRAMCs has been demonstrated by Zhang et al., and the schematic diagrams are presented in Fig. 6 [68]. As shown in Fig. 6(b), GNSs-rich tribofilms were smeared on the worn surface of the Al/GNSs composite during the sliding wear tests, and two effects of GNSs-rich tribofilms on the wear behavior were found. On one hand, the wrapping effect around wear debris and the bridging effect between subsurface cracks of GNSs can enhance the wear resistance of the composite (Figs. 6(c) and 6(d)). On the other hand, GNSs can act as a solid lubricant through interlayer sliding and formation of rollers (Figs. 6(e) and 6(f)), thereby leading to a lower COF value. Moreover, it should be noted that the self-lubricating effect cannot be obtained by incorporating single-layer graphene into Al due to the lack of interlayer sliding. Through a series of molecular dynamics simulations, Mohammadi et al. [70] found that the incorporation of single-layer graphene in Al matrix will even lead to a higher COF. The simulation results show that the plastic deformation in the front of the indenter is more severe for the Al/graphene composite due to the promoted dislocation movement in the Al/graphene coherent-like interfacial region. The intensive plastic deformation in the Al/graphene composite will result in a higher tangential force during the wear process. Thus, the COF value was elevated. Due to these reasons, the incorporation of GNPs/GNSs/FLG is more favorable for obtaining an attractive self-lubricating property.

According to previous studies, a stable mechanically mixed layer (MML) could be formed on the worn surface of GRAMCs during the wear tests [32,71–72]. The formation of MML can reduce the contact between the friction pair, thereby providing a protective effect to the worn surface. In our previous work, the effects of RGO on the tribological behavior of Al–Si/(SiC + RGO) composites were studied [71]. It was found that the COF of the composites was stabilized and the wear resistance was enhanced through the incorporation of RGO. The improvement in wear resistance of the Al–Si/(SiC + RGO) composites can be ascribed to three aspects: (i) strengthening effects of RGO; (ii) MML formation; and (iii) self-lubricating mechanism. The corresponding illustration of the wear mechanism of the Al–Si/(SiC + RGO) composites are presented in Fig. 7 [71]. As shown in Fig. 7(a), the major wear mechanism of Al–Si/SiC composites under all loads is delamination wear due to the lack of lubrication. For the Al–Si/(SiC + 0.5 wt.% RGO) composite, the presence of MML can effectively protect the worn surface from damage and provide a lubricating effect (Fig. 7(b)). Under lower loads, the wear mechanism of the Al–Si/(SiC + 0.5 wt.% RGO) composite was abrasive wear and local adhesion wear. For the Al–Si/(SiC + 0.7 wt.% RGO) composite, agglomeration of RGO within the composite occurred and thus deteriorated the plasticity of the

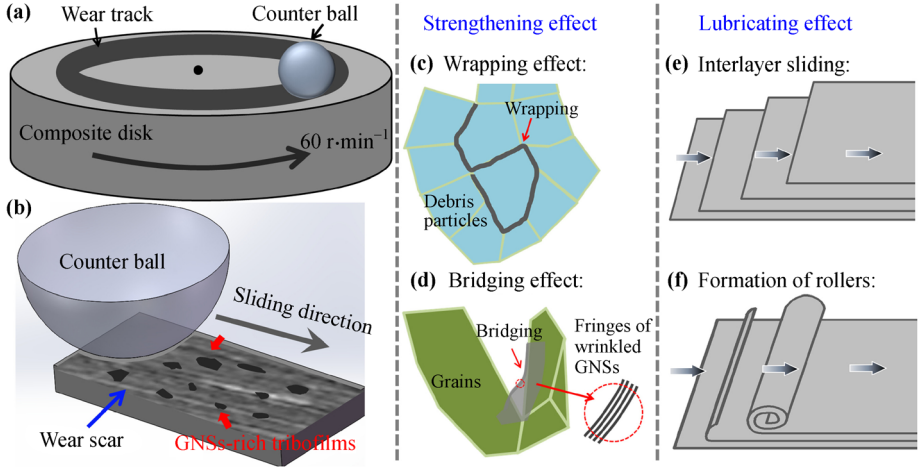

Fig. 6 Schematic diagrams of the effects of GNSs on the wear behavior: **(a)(b)** general view of the wear test; **(c)** wrapping effect of GNSs around wear debris; **(d)** bridging effect of GNSs between subsurface cracks; **(e)(f)** the self-lubricating mechanism of GNSs. Reproduced with permission from Ref. [68].

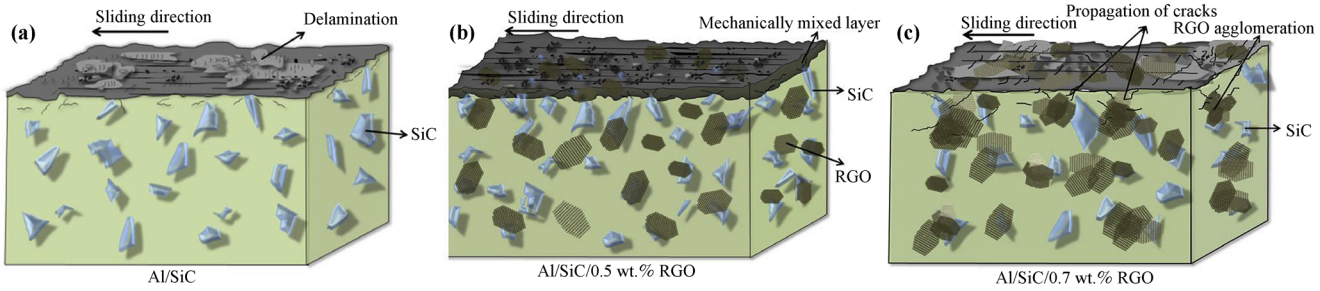

Fig. 7 Illustration of the wear mechanism: **(a)** Al–Si/SiC under all loads; **(b)** Al–Si/SiC/0.5 wt.% RGO under lower loads; **(c)** Al–Si/SiC/0.7 wt.% RGO under higher loads. Reproduced with permission from Ref. [71].

composite (Fig. 7(c)). At this point, the cracks perpendicular to composites was formed and severe delamination wear occurred during the wear tests, thereby leading to a weakened wear resistance.

3.2.2 Tribological properties

As discussed above, the tribological performance of the GRAMCs is generally more favorable than the unreinforced Al matrix. The tribological properties of various GRAMCs are summarized in Table 5 [32,41,68–69,71,73–74]. In general, the COF of GRAMCs decreased to some extent with relative to unreinforced alloy, which is attractive for industrial applications. Due to that the tribological performance is influenced by many factors, e.g., the test method, the counterface composition, the sliding velocity/frequency, the load and the temperature, it is unreasonable to compare tribological properties obtained from different studies. To present the results more concisely, we list the increment in tribological properties of GRAMCs with relative to the unreinforced alloy matrix.

3.3 Electrical properties

Due to the excellent EC of graphene (9.6×10^7 S·m^{-1}), the EC of GRAMCs is expected to be enhanced through the incorporation of graphene [10,75]. However, there are only a few studies reported an enhanced EC of GRAMCs relative to the corresponding alloy matrix [10,18,29,59,76]. The main restrictions to EC of GRAMCs come from two aspects: (i) the superior intrinsic EC of graphene relies on many factors, e.g., fabricating method, structural integrity and intrinsic defects; and (ii) the increment in EC is strongly dependent on the homogeneous dispersion of graphene and robust interfacial bonding between Al and graphene.

The influence of interface structure on the EC of GRAMCs is investigated by Cao et al. [10]. The current

Table 5 Tribological properties of recently developed GRAMCs [32,41,68–69,71,73–74]

Matrix	Reinforcement	Process	Tribological properties [a)]	Dominant wear mechanism [e)]	Ref.
AlSi10Mg	~1 wt.% GNPs	SLM	~42% increase in wear rate [b)]	abrasive wear for the composite	[32]
Al	0.5 wt.% GNPs	PM	70% decrease in COF, 67% decrease in wear rate [c)]	adhesive wear for both samples	[41]
A355	1 vol.% GNSs	PM	39% decrease in COF, 85% decrease in wear rate	abrasive and adhesive wear for both samples for the composite, with relatively weak abrasive wear due to a lower COF	[68]
Al6061	SiC + GNPs	FSP	> 20% decrease in COF, 56% decrease in wear rate	adhesive wear (matrix) and abrasive wear (composite)	[69]
Al–7Si/10SiC	0.5 wt.% RGO	PM	65% decrease in wear rate [d)]	delamination wear for Al–Si/SiC and abrasive wear for Al–Si/(SiC + RGO)	[71]
AA2124	3 wt.% graphene	PM	25% decrease in COF, 34% decrease in wear rate	abrasive wear for both samples	[73]
Al	0.1 wt.% GNPs	PM	no obvious change in COF, ~8% decrease in wear rate [c)]	abrasive wear for the composite	[74]
	1 wt.% GNPs	PM	~3% decrease in COF, ~24% increase in wear rate [c)]	abrasive wear for the composite	

Notes: COF, coefficient of friction; FSP, friction stir processing; GNP, graphene nanoplatelet; GNS, graphene nanosheet; GRAMC, graphene-reinforced aluminum matrix composite; PM, powder metallurgy; RGO, reduced graphene oxide; SLM, selective laser melting.
a) Relative to the corresponding alloy matrix; b) 20 N, 0.6 m·s^{-1}; c) At a load of 10 N; d) At a load of 1 N; e) For matrix and composite.

mapping results in this study revealed that the peak current intensity of the Al/graphene interface in the Al/graphene/Al sandwiched structure increased abruptly, and the maximum current (29.3 pA) was 73 times higher than that of the surrounding Al matrix. The significant increment in EC indicates that the GRAMCs possess excellent EC theoretically. However, the maximum current (29.3 pA) obtained in the study still far below its expected value, which could be attributed to the presence of amorphous alumina in the Al/graphene/Al interface, as shown in Fig. 8(a). The amorphous alumina formed during the fabricating process will inhibit the transfer of doped electrons from the Al matrix to graphene and enhances the scattering of charge carriers on phonons, thereby resulting in a weakened EC value. To further investigate the effect of alumina on the EC, a passivated Al/graphene/passivated Al interface was synthesized, as shown in Fig. 8(b). In the Al–O/graphene/O–Al interface, amorphous alumina layers (~4 nm) were formed between graphene and Al matrix, and the current mapping tests indicated that maximum current of Al–O/graphene/O–Al interface is less than 1.0 pA. The results demonstrated that the alumina impurities formed at the Al/graphene interface have an inhibitory effect on the EC of embedded graphene.

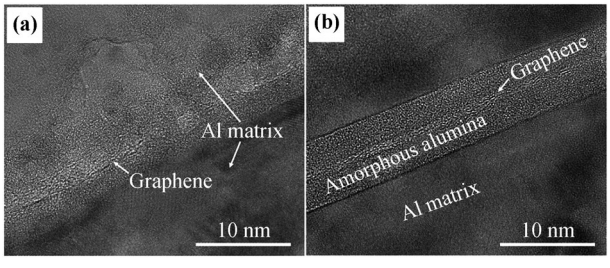

Fig. 8 TEM images of **(a)** Al/graphene/Al and **(b)** passivated Al/graphene/passivated Al. Reproduced with permission from Ref. [10].

Recently, Yu et al. [18] reported an elevated EC of the Al6063/GNSs composite relative to Al6063 alloy prepared by a ball milling combined with squeeze casting method. It should be noted that the EC of the composite is improved only when the milling time is 3 h, and longer or shorter milling time has no obvious effect on the EC. Due to the gas atomization Al powders usually accompanied by the introduction of oxidation film, the amorphous alumina film was observed at the interface between Al and GNSs at a short milling time (1 h), as shown by the high-resolution transmission electron microscopy (HRTEM) image in Fig. 9(a). By performing a longer milling time (3 h), the oxidation film was broken and direct contact between Al/GNSs was observed (Fig. 9(b)), thus, an elevated EC of the composite was obtained. Further extending the milling time to 4 h result in the formation of large quantities of insulating Al_4C_3 and damaged the structural integrity of graphene, thereby reducing the EC. According to EC measurements, the EC of the Al6063/GNSs composite was 52.9% IACS (international annealed copper standard) when the ball milling is 3 h, 17.4% higher than that of the corresponding Al6063 alloy matrix.

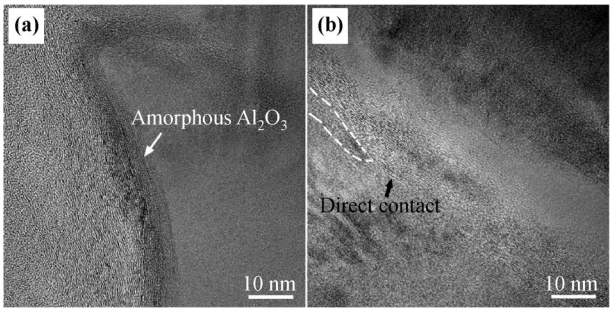

Fig. 9 HRTEM images of the interfacial area of Al6063/GNSs composites with **(a)** 1 h and **(b)** 3 h ball milling. Reproduced with permission from Ref. [18].

In summary, the direct contact and the strong interfacial bonding between Al and graphene are essential for achieving an elevated EC of GRAMCs. To obtaining an elevated EC, following factors should be taken into consideration: (i) ensuring the direct contact between Al and graphene; (ii) avoiding the formation of Al_2O_3 impurities and Al_4C_3 intermetallics; (iii) maintaining the structural integrity of graphene; and (iv) promoting the dispersion of graphene.

3.4 Thermal properties

To meet the requirements of elevated temperature applications, good thermal properties are essential for GRAMCs to prevent the heat accumulation that could damage the structural integrity. Generally, Al is considered a thermally conductive material (with a TC of 237 $W \cdot m^{-1} \cdot K^{-1}$), but the high CTE ($(21–24)\times10^{-6}$ K^{-1}) restricts its utilization in industrial applications. In previous studies, conventional ceramic reinforcements (e.g., SiC and TiB_2) were used to reduce the CTE of AMCs, while the TC generally decreased simultaneously. To overcome this contradiction, graphene is considered as a promising reinforcement phase for AMCs due to its superior high TC and negative CTE (TC: 1000–5300 $W \cdot m^{-1} \cdot K^{-1}$ (in-plane), CTE: -6×10^{-6}

K^{-1}) [9,17,77]. However, the excellent TC of graphene is directional dependent [77–78]. The in-plane TC of graphene is significantly higher than the through-plane TC (5–20 $W \cdot m^{-1} \cdot K^{-1}$). Thus, the TC of GRAMCs can only be enhanced in the alignment direction of graphene reinforcements [78–79].

Zhang et al. [80] fabricated the Al/RGO composite through PM and investigated its thermal properties. By adding 0.3 wt.% graphene into the Al matrix, the TC and the specific heat capacity of the composite were increased by 15.4% and 9.1%, respectively. The improvement in TC was ascribed to the extremely high TC of graphene and the robust interfacial bonding between Al/graphene.

Tiwari et al. [81] synthesized Al/bilayer graphene composite by a hot accumulative roll bonding method. Through accumulative roll bonding processing, the TC of annealed Al was reduced by ~17% due to the grain refinement. However, the decrease in TC can be recovered with the incorporation of 0.1 wt.% graphene, which can be attributed to the existence of thermal boundary conductance of the Al/graphene interface that increases the TC of the Al/bilayer graphene composites.

4 Challenges and corresponding strategy related to GRAMCs

4.1 Inhomogeneous dispersion

As discussed above, graphene possesses a huge specific surface area, resulting in a tendency to agglomerate within the Al matrix. In previous studies, inhomogeneous dispersion of graphene occurred in many cases, especially when the content of graphene is high (>2 wt.%) [82]. Main reasons for the inhomogeneous dispersion include the existence of the van der Waals interaction among GNSs and the poor wettability between Al and graphene. The agglomeration of graphene not only weakens its strengthening effects, but also generates defects at the Al/graphene interface, harmful to the comprehensive performance of GRAMCs. Specifically, the graphene agglomerations will act as crack-initiation sites during plastic deformation, thus leading to the premature failure of the composites.

Conventional mixing methods, such as solution mixing and ball milling, are discussed in Section 2.1. These methods are aimed at breaking the van der Waals interaction between GNSs by ball milling/ultrasonic/stirring to achieve uniform dispersion. Through appropriate mixing parameters, a balance between the uniform dispersion and the structural integrity of graphene can be achieved. Benefiting from high production rate and cost-effectiveness, these methods are promising for industrial applications [18]. However, these methods cannot improve the wettability between Al and graphene, so the dispersibility of graphene is still limited.

To improve the wettability between Al and graphene, coating a metallic layer (e.g., Ni and Cu) on graphene, decorating graphene with metal nanoparticles (MNPs), and forming intermetallics (e.g., Al_3Ni, Al_3Ni_2, and Al_2Cu) are all proven to be feasible methods [46,53]. Moreover, these methods can prevent the carbide formation by inhibiting the interfacial reactions between Al and graphene [49]. In addition, the addition of alloying elements into Al can bring solid solution strengthening and precipitation strengthening, thus achieving higher mechanical properties. The chemical reduction, electroless plating, molecular lever mixing (MLM), and *in-situ* chemical vapor deposition (CVD) are commonly used methods for modifying graphene with MNPs or metallic layers [49,53,61]. Guan et al. [45] incorporated Ni into Al/Ni-coated GNSs composites through a PM method, and the results indicated that not only the dispersion of GNSs was promoted, but also the carbide formation was suppressed. Bhadauria et al. [51] fabricated homogeneously dispersed GNPs/Al composites through a combined chemical functionalization, physical functionalization, liquid mixing and SPS method. By incorporating 0.5 wt.% physio-chemically functionalized GNPs into the Al matrix, the UTS of the composite was enhanced by 63% relative to monolithic Al. Han et al. [49] reported a bottom-up strategy based on the spray-drying and high-temperature CVD techniques, and synthesized Ni MNPs-modified GNPs (Ni-GNPs) and Cu MNPs-modified GNPs (Cu-GNPs) through this strategy. Through the incorporation of Ni-GNPs or Cu-GNPs into GRAMCs, the homogeneous dispersion of GNPs in GRAMCs was obtained. Khoshghadam-Pireyyousefan et al. [53] synthesized Al–4Cu/RGO composites through a novel MLM followed by the SPS method. Benefiting from the uniform dispersion of RGO and robust interfacial bonding between Al and RGO, a significant improvement in mechanical properties of the composites was obtained. YTS and UTS values of the Al–4Cu/1 wt.% RGO composite were increased by 79% and 49% with relative to those of the Al–4Cu alloy, respectively.

In addition to these chemical methods, the secondary processing approaches such as hot rolling, hot extrusion and FSP are also effective for promoting the dispersion of

graphene [83]. For instance, Zhang et al. [42] fabricated the Al2009/1 wt.% GNPs composite through PM followed by multi-pass FSP route. Microstructural observation revealed that the dispersion of GNPs was significantly improved with the increasing FSP passes. After two FSP passes, the GNPs were dispersed within the Al matrix uniformly and the mechanical properties were enhanced effectively. YTS and UTS values of the 2-pass FSP composite were 398 and 514 MPa, which were 30.5% and 23.3% higher than those of the Al2009 alloy, respectively.

4.2 Weak interfacial bonding and carbide formation

Compared with conventional AMCs, GRAMCs is characterized by the large volume fraction of the matrix/reinforcement interface area. Thus, enhancing the interface bonding between graphene and Al is the core issue to achieve a more favorable performance of GRAMCs. However, the interfacial bonding between Al and graphene is naturally weak due to that the bonding is applied by the weak van der Waals force [84]. The weak van der Waals force is insufficient to realize high load transfer efficiency, thereby leading to a very limited strengthening effect [85]. One of the feasible methods for achieving strong interfacial bonding is introducing appropriate interfacial reactions between Al and C, leading to the interfacial bonding transformed from weak mechanical bonding to strong chemical bonding [75]. As shown in Fig. 10, compared with the weak mechanical bonding, the strong chemical bonding between the reinforcement and the alloy matrix is more favorable for the load transfer effect [50].

Due to the low Gibbs free energy of the Al_4C_3 formation (-196 kJ·mol^{-1} at 298 K), the Al_4C_3 phase is generally formed within GRAMCs through the chemical reaction between Al and C [86]. Interestingly, the effects of Al_4C_3 on mechanical properties of GRAMCs are controversial in different studies. Zhou et al. [75] proposed that the appropriate interfacial reaction between Al/C is favorable to the mechanical properties, while overreaction is harmful. In their study, the Al_4C_3 nanorods generated at the Al/FLG interface ensured an efficient load transfer and thereby leading to higher mechanical properties. Jiang et al. [64] reported that a tight Al/GNS interface without the formation of Al_4C_3 is most favorable to the mechanical properties of GRAMCs. Guo et al. [87] proposed that the role of Al_4C_3 on the mechanical properties of Al/CNTs composites is size-dependent, i.e., nano-sized Al_4C_3 enhances the strength of composites, while micro-sized Al_4C_3 deteriorates the strength.

The graphene edges are more reactive and defective than its basal-plane due to the presence of rich carbon dangling bonds [88]. Thus, the Al_4C_3 phase is preferred nucleate at the graphene edges. Moreover, the graphene defects are also preferential sites for the Al_4C_3 formation [89–90]. This indicates that the formation of Al_4C_3 can be effectively controlled by changing the structural integrity, size and shape of graphene. Jiang et al. [90] investigated the nucleation and growth mechanisms of Al_4C_3 intermetallics in the Al/GNSs composites. As presented in Fig. 11, for the Al_4C_3/Al interface, the Al_4C_3 phase was commonly formed either along or at an angle to the Al grain boundary, and four orientation relationships between Al and Al_4C_3 intermetallics were found: (i) ~25° between $Al_4C_3(0\ 0\ 3)$ and $Al(\bar{1}\ 1\ 1)$; (ii) $Al_4C_3(0\ 0\ 3)$//$Al(1\ \bar{1}\ 1)$; (iii) $Al_4C_3(0\ 0\ 3)$//$Al(0\ 0\ 2)$; (iv) $Al_4C_3(0\ 0\ 3)$//$Al(2\ \bar{2}\ 0)$. The proportions of such four orientation relationships are

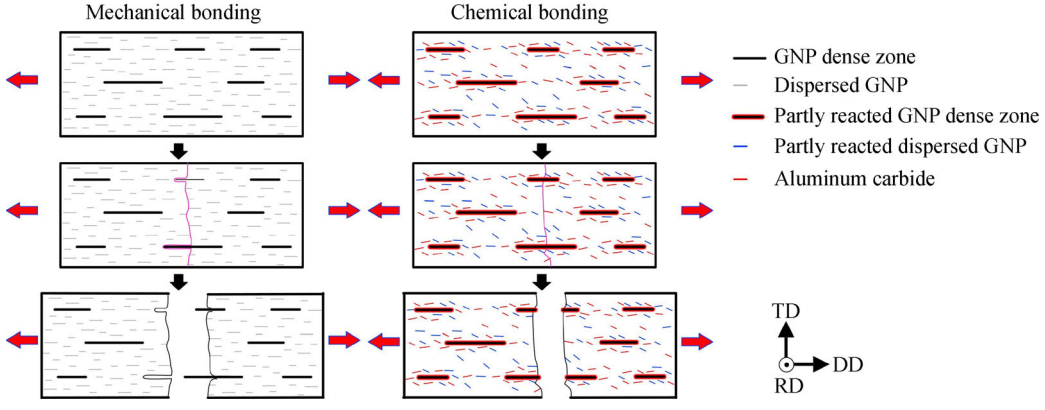

Fig. 10 Illustrations of the tensile behavior of Al/GNP composites with weak mechanical bonding and strong chemical bonding. Reproduced with permission from Ref. [50].

calculated to be 10.98%, 8.09%, 2.37% and 13.52%, respectively. Owing to the semi-coherency of these interfaces, Al_4C_3 can nucleate on the Al matrix under the above orientation relationships. This demonstrates that the interfacial bonding of GRAMCs could be enhanced by varying the preferred orientation of the Al matrix.

Modification of interfacial microstructure has been carried out to enhance the interfacial bonding in GRAMCs by Ju et al. [84]. In their study, polydimethylsiloxane was adopted as the PCA to tailor the interfacial microstructure during the ball milling process, and the Al/GNPs composites with the interface structure of graphene–Al_2O_3–Al and graphene–(Al_4C_3, Al_2OC)–Al were fabricated by pressure infiltration. Owing to the existence of PCA, the direct contact of Al/graphene is avoided, and the interfacial reaction products of GRAMCs were transformed from Al_4C_3 and Al_2OC to Al_2O_3. According to the first principle calculation, the shear strength of the Al_2O_3/graphene interface was 378 MPa, which was much stronger than those of Al_4C_3/graphene (83 MPa), Al_2OC/graphene (66 MPa) and Al/graphene (37 MPa). The mechanical tests demonstrated that the UTS of the composite with graphene–Al_2O_3–Al interfacial bonding was 30% higher than those with Al_4C_3 and Al_2OC interface. These findings provide a theoretical basis for enhancing the interfacial bonding by interfacial modification.

4.3 Structural integrity

The strengthening efficiency of graphene is strongly influenced by its structural integrity. Preservation of the graphene structural integrity is favorable to obtain high load transfer efficiency during the loading process [15,91]. However, the structure of graphene is inevitably damaged to some extent during the fabricating process, and the destruction of the graphene structure is usually accompanied by the formation of Al_4C_3. For maintaining the structural integrity of graphene, the feasible and economical way is to adopt mild sonication parameters and ball milling parameters during the mixing stage. Besides, a lower processing temperature also contributes to keeping the structural integrity of graphene and inhibiting the carbide formation. Moreover, *in-situ* CVD is also considered as an effective approach to maintain the integrity of graphene.

5 Concluding remarks and outlook

Graphene possesses various superior properties, such as extremely high elastic modulus and strength, and excellent EC and TC. Due to these attractive characteristics of graphene, the research related to GRAMCs grew vigorously in recent years. In this paper, we reviewed recent progress in the fabrication of GRAMCs and their properties. Generally, the fabrication methods of GRAMCs include PM, casting, SPD, and additive manufacturing. Among them, PM is most frequently used due to the uniform dispersion of reinforcements and mass production. Owing to the excellent mechanical properties and high wear resistance, GRAMCs are promising for structural applications. In terms of physical properties, the enhanced TC and EC and the decreased CTE of GRAMCs have also been reported relative to the unreinforced alloy matrix. In addition, the challenges and corresponding strategies related to GRAMCs are discussed, including inhomogeneous dispersion of graphene, weak interfacial bonding, carbide formation, and structural integrity. To overcome those challenges, researchers have developed many novel strategies for achieving higher performance of GRAMCs. Nevertheless, the mechanical and physical properties achieved are still far below theoretically predicted ones, indicating that there is still much room for the improvement of the GRAMC performance. With the development of

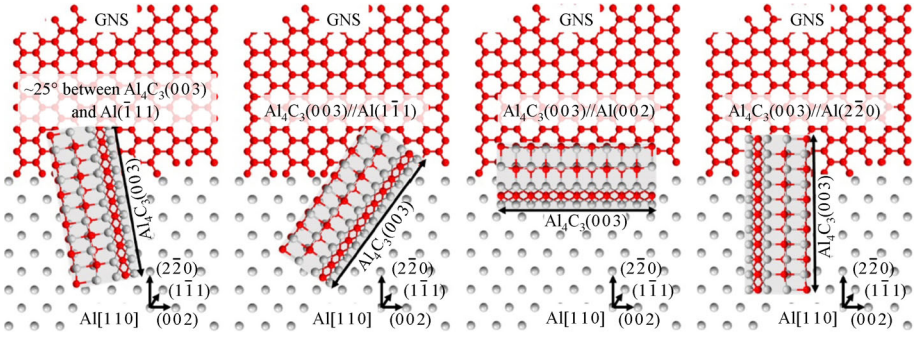

Fig. 11 Schematic diagrams of the nucleation and the growth mechanisms of Al_4C_3. Reproduced with permission from Ref. [90].

fabrication methods and the further deepening of research, GRAMCs are expected to have broad prospects in industrial applications.

Acknowledgements This work was supported by the National Natural Science Foundation of China (Grant No. 51774124) and the Natural Science Foundation of Hunan Province (Grant No. 2019JJ40017).

References

[1] Chen S, Teng J, Luo H, et al. Hot deformation characteristics and mechanism of PM 8009Al/SiC particle reinforced composites. Materials Science & Engineering A, 2017, 697: 194–202

[2] Chen S, Fu D, Luo H, et al. Hot workability of PM 8009Al/Al_2O_3 particle-reinforced composite characterized using processing maps. Vacuum, 2018, 149: 297–305

[3] Bo G, Jiang F, Dong Z, et al. Revealing the influence of pre-precipitation microstructure on hot workability in an Al–Cu–Mg–Zr alloy. Materials Science & Engineering A, 2019, 755: 147–157

[4] ASM Handbook Volume 02: Properties and Selection: Nonferrous Alloys and Special-Purpose Materials. ASM International, 1990

[5] Zhu Y, Murali S, Cai W, et al. Graphene and graphene oxide: Synthesis, properties, and applications. Advanced Materials, 2010, 22(35): 3906–3924

[6] Lee C, Wei X, Kysar, J W, et al. Measurement of the elastic properties and intrinsic strength of monolayer graphene. Science, 2008, 321(5887): 385–388

[7] Balandin A A, Ghosh S, Bao W, et al. Superior thermal conductivity of single-layer graphene. Nano Letters, 2008, 8(3): 902–907

[8] Liu J. Charging graphene for energy. Nature Nanotechnology, 2014, 9(10): 739–741

[9] Yoon D, Son Y W, Cheong H. Negative thermal expansion coefficient of graphene measured by Raman spectroscopy. Nano Letters, 2011, 11(8): 3227–3231

[10] Cao M, Luo Y Z, Xie Y Q, et al. The influence of interface structure on the electrical conductivity of graphene embedded in aluminum matrix. Advanced Materials Interfaces, 2019, 6(13): 1900468

[11] Moghadam A D, Omrani E, Menezes P L, et al. Mechanical and tribological properties of self-lubricating metal matrix nanocomposites reinforced by carbon nanotubes (CNTs) and graphene — A review. Composites Part B: Engineering, 2015, 77: 402–420

[12] Awotunde M A, Adegbenjo A O, Obadele B A, et al. Influence of sintering methods on the mechanical properties of aluminium nanocomposites reinforced with carbonaceous compounds: A review. Journal of Materials Research and Technology, 2019, 8(2): 2432–2449

[13] Dixit S, Mahata A, Mahapatra D R, et al. Multi-layer graphene reinforced aluminum — Manufacturing of high strength composite by friction stir alloying. Composites Part B: Engineering, 2018, 136: 63–71

[14] Dasari B L, Morshed M, Nouri J M, et al. Mechanical properties of graphene oxide reinforced aluminium matrix composites. Composites Part B: Engineering, 2018, 145: 136–144

[15] Pourmand N S, Asgharzadeh H. Aluminum matrix composites reinforced with graphene: A review on production, microstructure, and properties. Critical Reviews in Solid State and Material Sciences, 2019, 45(4): 289–337

[16] Lu A, Zhao L, Liu Y, et al. Enhanced damping capacity in graphene–Al nanolaminated composite pillars under compression cyclic loading. Metallurgical and Materials Transactions A: Physical Metallurgy and Materials Science, 2020, 51(4): 1463–1468

[17] Han T, Li J, Zhao N, et al. Microstructure and properties of copper coated graphene nanoplates reinforced Al matrix composites developed by low temperature ball milling. Carbon, 2020, 159: 311–323

[18] Yu Z, Yang W, Zhou C, et al. Effect of ball milling time on graphene nanosheets reinforced Al6063 composite fabricated by pressure infiltration method. Carbon, 2019, 141: 25–39

[19] Akçamli N, Küçükelyas B, Kaykilarli C, et al. Investigation of microstructural, mechanical and corrosion properties of graphene nanoplatelets reinforced Al matrix composites. Materials Research Express, 2019, 6(11): 115627

[20] Zeng X, Teng J, Yu J, et al. Fabrication of homogeneously dispersed graphene/Al composites by solution mixing and powder metallurgy. International Journal of Minerals Metallurgy and Materials, 2018, 25(1): 102–109

[21] Huang C Y, Hu S P, Chen K. Influence of rolling temperature on the interfaces and mechanical performance of graphene-reinforced aluminum-matrix composites. International Journal of Minerals Metallurgy and Materials, 2019, 26(6): 752–759

[22] Prakash P B, Raju K B, Venkatasubbaiah K, et al. Microstructure analysis and evaluation of mechanical properties of Al 7075 GNP's composites. Materials Today: Proceedings, 2018, 5(6): 14281–14291

[23] Dong Y F, Ren B H, Wang K, et al. Effects of graphene addition on the microstructure of 7075Al. Materials Research Express, 2020, 7(2): 026510

[24] Venkatesan S, Xavior M A. Characterization on aluminum alloy 7050 metal matrix composite reinforced with graphene nanoparticles. In: Procedia Manufacturing, 2019, 30: 120–127

[25] Das S, Kordijazi A, Akbarzadeh O, et al. An innovative process for dispersion of graphene nanoparticles and nickel spheres in A356 alloy using pressure infiltration technique. Engineering

Reports, 2020, 2: 1–7

[26] Sharma A, Sharma V M, Sahoo B, et al. Effect of multiple micro channel reinforcement filling strategy on Al6061–graphene nanocomposite fabricated through friction stir processing. Journal of Manufacturing Processes, 2019, 37: 53–70

[27] Zare H, Jahedi M, Toroghinejad M R, et al. Compressive, shear, and fracture behavior of CNT reinforced Al matrix composites manufactured by severe plastic deformation. Materials & Design, 2016, 106: 112–119

[28] Kumar A P, Madhu H C, Pariyar A, et al. Friction stir processing of squeeze cast A356 with surface compacted graphene nanoplatelets (GNPs) for the synthesis of metal matrix composites. Materials Science & Engineering A, 2020, 769: 138517

[29] Huang Y, Bazarnik P, Wan D, et al. The fabrication of graphene-reinforced Al-based nanocomposites using high-pressure torsion. Acta Materialia, 2019, 164: 499–511

[30] Li Y, Feng Z, Huang L, et al. Additive manufacturing high performance graphene-based composites: A review. Composites Part A: Applied Science and Manufacturing, 2019, 124: 105483

[31] Hu Z, Chen F, Xu J, et al. 3D printing graphene–aluminum nanocomposites. Journal of Alloys and Compounds, 2018, 746: 269–276

[32] Wu L, Zhao Z, Bai P, et al. Wear resistance of graphene nanoplatelets (GNPs) reinforced AlSi10Mg matrix composite prepared by SLM. Applied Surface Science, 2020, 503: 144156

[33] Tiwari J K, Mandal A, Sathish N, et al. Investigation of porosity, microstructure and mechanical properties of additively manufactured graphene reinforced AlSi10Mg composite. Additive Manufacturing, 2020, 33: 101095

[34] Zhou W W, Dong M Q, Zhou Z X, et al. *In situ* formation of uniformly dispersed Al_4C_3 nanorods during additive manufacturing of graphene oxide/Al mixed powders. Carbon, 2019, 141: 67–75

[35] Zhao Z Y, Bai P K, Misra R D K, et al. AlSi10Mg alloy nanocomposites reinforced with aluminum-coated graphene: Selective laser melting, interfacial microstructure and property analysis. Journal of Alloys and Compounds, 2019, 792: 203–214

[36] Zhao Z Y, Misra R D K, Bai P K, et al. Novel process of coating Al on graphene involving organic aluminum accompanying microstructure evolution. Materials Letters, 2018, 232: 202–205

[37] Zhao W, Zhao Z, Bai P, et al. The interfacial characteristics of graphene/Al_4C_3 in graphene/AlSi10Mg composites prepared by selective laser melting: First principles and experimental results. Materials, 2020, 13(3): 702

[38] Kelly A, Tyson W R. Tensile properties of fibre-reinforced metals: Copper/tungsten and copper/molybdenum. Journal of the Mechanics and Physics of Solids, 1965, 13(6): 329–350

[39] Zhang Z, Chen D L. Consideration of Orowan strengthening effect in particulate-reinforced metal matrix nanocomposites: A model for predicting their yield strength. Scripta Materialia, 2006, 54(7): 1321–1326

[40] Wang J, Li Z, Fan G, et al. Reinforcement with graphene nanosheets in aluminum matrix composites. Scripta Materialia, 2012, 66(8): 594–597

[41] Islam M, Khalid Y, Ahmad I, et al. Microstructural evaluation of inductively sintered aluminum matrix nanocomposites reinforced with silicon carbide and/or graphene nanoplatelets for tribological applications. Metallurgical and Materials Transactions A: Physical Metallurgy and Materials Science, 2018, 49A(7): 2963–2976

[42] Zhang Z W, Liu Z Y, Xiao B L, et al. High efficiency dispersal and strengthening of graphene reinforced aluminum alloy composites fabricated by powder metallurgy combined with friction stir processing. Carbon, 2018, 135: 215–223

[43] Li J C, Zhang X X, Geng L. Improving graphene distribution and mechanical properties of GNP/Al composites by cold drawing. Materials & Design, 2018, 144: 159–168

[44] Jiang Y Y, Xu R, Tan Z Q, et al. Interface-induced strain hardening of graphene nanosheet/aluminum composites. Carbon, 2019, 146: 17–27

[45] Guan R, Wang Y, Zheng S, et al. Fabrication of aluminum matrix composites reinforced with Ni-coated graphene nanosheets. Materials Science & Engineering A, 2019, 754: 437–446

[46] Wang J, Zhang X, Zhao N, et al. *In situ* synthesis of copper-modified graphene-reinforced aluminum nanocomposites with balanced strength and ductility. Journal of Materials Science, 2019, 54(7): 5498–5512

[47] Hsieh C T, Ho Y C, Wang H H, et al. Mechanical and tribological characterization of nanostructured graphene sheets/A6061 composites fabricated by induction sintering and hot extrusion. Materials Science & Engineering A, 2020, 786: 138998

[48] Li M, Zhang Z, Gao H, et al. Formation of multilayer interfaces and the load transfer in graphene nanoplatelets reinforced Al matrix composites. Materials Characterization, 2020, 159: 110018

[49] Han T L, Liu E Z, Li J J, et al. A bottom-up strategy toward metal nano-particles modified graphene nanoplates for fabricating aluminum matrix composites and interface study. Journal of Materials Science & Technology, 2020, 46: 21–32

[50] Li J C, Zhang X X, Geng L. Effect of heat treatment on interfacial bonding and strengthening efficiency of graphene in GNP/Al composites. Composites Part A: Applied Science and Manufacturing, 2019, 121: 487–498

[51] Bhadauria A, Singh L K, Laha T. Effect of physio-chemically functionalized graphene nanoplatelet reinforcement on tensile properties of aluminum nanocomposite synthesized via spark plasma sintering. Journal of Alloys and Compounds, 2018, 748: 783–793

[52] Bhadauria A, Singh L K, Laha T. Combined strengthening effect of nanocrystalline matrix and graphene nanoplatelet reinforcement on the mechanical properties of spark plasma sintered aluminum based nanocomposites. Materials Science & Engineering A, 2019, 749: 14–26

[53] Khoshghadam-Pireyousefan M, Rahmanifard R, Orovcik L, et al. Application of a novel method for fabrication of graphene reinforced aluminum matrix nanocomposites: Synthesis, microstructure, and mechanical properties. Materials Science & Engineering A, 2020, 772: 138820

[54] Li P, Chen L, Cao B, et al. Hierarchical microstructure architecture: A roadmap towards strengthening and toughening reduced graphene oxide/2024Al matrix composites synthesized by flake powder thixoforming. Journal of Alloys and Compounds, 2020, 823: 153815

[55] Li M, Gao H Y, Liang J M, et al. Microstructure evolution and properties of graphene nanoplatelets reinforced aluminum matrix composites. Materials Characterization, 2018, 140: 172–178

[56] Shao P Z, Yang W S, Zhang Q, et al. Microstructure and tensile properties of 5083 Al matrix composites reinforced with graphene oxide and graphene nanoplates prepared by pressure infiltration method. Composites Part A: Applied Science and Manufacturing, 2018, 109: 151–162

[57] Shao P Z, Chen G Q, Ju B Y, et al. Effect of hot extrusion temperature on graphene nanoplatelets reinforced Al6061 composite fabricated by pressure infiltration method. Carbon, 2020, 162: 455–464

[58] Sharma A, Sharma V M, Paul J. Fabrication of bulk aluminum–graphene nanocomposite through friction stir alloying. Journal of Composite Materials, 2020, 54(1): 45–60

[59] Zhang S, Chen G Q, Qu T M, et al. Simultaneously enhancing mechanical properties and electrical conductivity of aluminum by using graphene as the reinforcement. Materials Letters, 2020, 265: 127440

[60] Xie Y M, Meng X C, Huang Y X, et al. Deformation-driven metallurgy of graphene nanoplatelets reinforced aluminum composite for the balance between strength and ductility. Composites Part B: Engineering, 2019, 177: 107413

[61] Liu X H, Li J J, Sha J W, et al. *In-situ* synthesis of graphene nanosheets coated copper for preparing reinforced aluminum matrix composites. Materials Science & Engineering A, 2018, 709: 65–71

[62] Liu X H, Li J J, Liu E Z, et al. Towards strength–ductility synergy with favorable strengthening effect through the formation of a quasi-continuous graphene nanosheets coated Ni structure in aluminum matrix composite. Materials Science & Engineering A, 2019, 748: 52–58

[63] Pu B W, Sha J W, Liu E Z, et al. Synergistic effect of Cu on laminated graphene nanosheets/AlCu composites with enhanced mechanical properties. Materials Science & Engineering A, 2019, 742: 201–210

[64] Jiang Y Y, Tan Z Q, Fan G L, et al. Reaction-free interface promoting strength–ductility balance in graphene nanosheet/Al composites. Carbon, 2020, 158: 449–455

[65] Archard J F. Contact and rubbing of flat surfaces. Journal of Applied Physics, 1953, 24(8): 981–988

[66] Xia H M, Zhang L, Zhu Y C, et al. Mechanical properties of graphene nanoplatelets reinforced 7075 aluminum alloy composite fabricated by spark plasma sintering. International Journal of Minerals Metallurgy and Materials, 2020, 27(9): 1295–1300

[67] Baig Z, Mamat O, Mustapha M, et al. Surfactant-decorated graphite nanoplatelets (GNPs) reinforced aluminum nanocomposites: Sintering effects on hardness and wear. International Journal of Minerals Metallurgy and Materials, 2018, 25(6): 704–715

[68] Zhang J S, Chen Z X, Wu H, et al. Effect of graphene on the tribolayer of aluminum matrix composite during dry sliding wear. Surface & Coatings Technology, 2019, 358: 907–912

[69] Sharma A, Sharma V M, Paul J. A comparative study on microstructural evolution and surface properties of graphene/CNT reinforced Al6061–SiC hybrid surface composite fabricated via friction stir processing. Transactions of Nonferrous Metals Society of China, 2019, 29(10): 2005–2026

[70] Mohammadi S, Montazeri A, Urbassek H M. Geometrical aspects of nanofillers influence the tribological performance of Al-based nanocomposites. Wear, 2020, 444: 203117

[71] Zeng X, Yu J G, Fu D F, et al. Wear characteristics of hybrid aluminum matrix composites reinforced with well-dispersed reduced graphene oxide nanosheets and silicon carbide particulates. Vacuum, 2018, 155: 364–375

[72] Reddy A P, Krishna P V, Rao R N. Tribological behaviour of Al6061–2SiC–*x*Gr hybrid metal matrix nanocomposites fabricated through ultrasonically assisted stir casting technique. Silicon, 2019, 11(6): 2853–2871

[73] El-Ghazaly A, Anis G, Salem H G. Effect of graphene addition on the mechanical and tribological behavior of nanostructured AA2124 self-lubricating metal matrix composite. Composites Part A: Applied Science and Manufacturing, 2017, 95: 325–336

[74] Tabandeh-Khorshid M, Omrani E, Menezes P L, et al. Tribological performance of self-lubricating aluminum matrix nanocomposites: Role of graphene nanoplatelets. Engineering Science and Technology: An International Journal, 2016, 19(1): 463–469

[75] Zhou W W, Mikulova P, Fan Y C, et al. Interfacial reaction induced efficient load transfer in few-layer graphene reinforced Al matrix composites for high-performance conductor. Composites Part B: Engineering, 2019, 167: 93–99

[76] Khan M, Din R U, Wadood A, et al. Effect of graphene

nanoplatelets on the physical and mechanical properties of Al6061 in fabricated and T6 thermal conditions. Journal of Alloys and Compounds, 2019, 790: 1076–1091

[77] Chu K, Wang X H, Li Y B, et al. Thermal properties of graphene/metal composites with aligned graphene. Materials & Design, 2018, 140: 85–94

[78] Wang J, Li J J, Weng G J, et al. The effects of temperature and alignment state of nanofillers on the thermal conductivity of both metal and nonmetal based graphene nanocomposites. Acta Materialia, 2020, 185: 461–473

[79] Balandin A A. Thermal properties of graphene and nanostructured carbon materials. Nature Materials, 2011, 10(8): 569–581

[80] Zhang L, Hou G M, Zhai W, et al. Aluminum/graphene composites with enhanced heat-dissipation properties by *in-situ* reduction of graphene oxide on aluminum particles. Journal of Alloys and Compounds, 2018, 748: 854–860

[81] Tiwari J K, Mandal A, Rudra A, et al. Evaluation of mechanical and thermal properties of bilayer graphene reinforced aluminum matrix composite produced by hot accumulative roll bonding. Journal of Alloys and Compounds, 2019, 801: 49–59

[82] Chen F, Gupta N, Behera R K, et al. Graphene-reinforced aluminum matrix composites: A review of synthesis methods and properties. JOM, 2018, 70(6): 837–845

[83] Mei Y, Shao P Z, Sun M, et al. Deformation treatment and microstructure of graphene reinforced metal-matrix nanocomposites: A review of graphene post-dispersion. International Journal of Minerals Metallurgy and Materials, 2020, 27(7): 888–899

[84] Ju B Y, Yang W S, Shao P Z, et al. Effect of interfacial microstructure on the mechanical properties of GNPs/Al composites. Carbon, 2020, 162: 346–355

[85] Asgharzadeh H, Sedigh M. Synthesis and mechanical properties of Al matrix composites reinforced with few-layer graphene and graphene oxide. Journal of Alloys and Compounds, 2017, 728: 47–62

[86] Laha T, Kuchibhatla S, Seal S, et al. Interfacial phenomena in thermally sprayed multiwalled carbon nanotube reinforced aluminum nanocomposite. Acta Materialia, 2007, 55(3): 1059–1066

[87] Guo B S, Chen B, Zhang X M, et al. Exploring the size effects of Al_4C_3 on the mechanical properties and thermal behaviors of Al based composites reinforced by SiC and carbon nanotubes. Carbon, 2018, 135: 224–235

[88] Banhart F, Kotakoski J, Krasheninnikov A V. Structural defects in graphene. ACS Nano, 2011, 5(1): 26–41

[89] Chu K, Wang F, Wang X H, et al. Interface design of graphene/copper composites by matrix alloying with titanium. Materials & Design, 2018, 144: 290–303

[90] Jiang Y Y, Tan Z Q, Fan G L, et al. Nucleation and growth mechanisms of interfacial carbide in graphene nanosheet/Al composites. Carbon, 2020, 161: 17–24

[91] Tabandeh-Khorshid M, Kumar A, Omrani E, et al. Synthesis, characterization, and properties of graphene reinforced metal-matrix nanocomposites. Composites Part B: Engineering, 2020, 183: 107664